Thermal hysteresis in the dielectric response of the charge density wave system o-TaS3

D. Starešinić, D. Dominko, Peter Lunkenheimer, Alois Loidl

Angaben zur Veröffentlichung / Publication details:

Starešinić, D., D. Dominko, Peter Lunkenheimer, and Alois Loidl. 2008. "Thermal hysteresis in the dielectric response of the charge density wave system o-TaS3." Journal of Physics: Condensed Matter 20 (44): 445231. https://doi.org/10.1088/0953-8984/20/44/445231.

Thermal hysteresis in the dielectric response of the charge density wave system o-TaS_3

D Starešinić[1,2], D Dominko[1], P Lunkenheimer[2] and A Loidl[2]

[1] Institute of Physics, HR-10001 Zagreb, POB 304, Croatia
[2] Experimental Physics V, Center for Electronic Correlations and Magnetism, University of Augsburg, D-86135 Augsburg, Germany

E-mail: damirs@ifs.hr

Abstract
The low frequency dielectric response of the charge density wave (CDW) system o-TaS_3 exhibits a rate-independent hysteresis on temperature cycling in a very wide temperature range below the CDW transition temperature. The ac conductivity, related to the CDW dynamics, is higher on heating than on cooling, while the dc conductivity of residual free carriers is lower, indicating a nontrivial relation between the two of them. Both the amplitude and the relaxation time of the low frequency relaxation process observed in the temperature region of the hysteresis are higher on heating, with similar temperature dependence to the hysteresis in the dc resistivity. The results indicate that the hystereses in ac and dc conductivities are mainly coupled through the free carrier screening of the CDW phase and not through the conversion of free carriers into phase defects.

1. Introduction

A charge density wave (CDW) is a broken symmetry ground state characterized by a periodic electron density modulation and lattice distortion which occurs in a number of anisotropic metallic systems with quasi one-dimensional electronic dispersion [1]. Typically, below the CDW transition temperature T_P, CDW systems become semiconducting as the new periodicity with the wavevector $q_{\mathrm{CDW}} = 2k_{\mathrm{F}}$ opens a gap at the Fermi surface. The new state exhibits a number of extraordinary phenomena such as nonlinear conductivity at low applied voltages (CDW sliding), narrow band noise in nonlinear regime and giant dielectric constant. They are due to the weak, but finite coupling of the CDW superstructure to the random defects in the underlying lattice, known as pinning, which makes the phase of the complex CDW parameter spatially non-uniform and correlated only on relatively short distances of the order of 1 μm, within so-called phase domains.

One of such puzzling feature of the CDW systems is the thermal hysteresis, which is observed in a wide temperature range below T_P, typically in the dc conductivity [2–5], but also in thermopower [6, 7], thermal expansion [8] or IR transmission [9] measurements. It has been considered as an indirect sign of different configurations of the randomly pinned CDW on cooling and heating, revealed due to the coupling of the CDW to the free carriers (dc conductivity, thermopower, IR transmission) or to the lattice (thermal expansion).

Hysteretic behaviour is commonly observed in ferroic (ferroelectric, ferromagnetic) systems [10] on the reversal of the appropriate external field, as there is a finite field required to reverse the direction of the macroscopic polarization. However, a thermal hysteresis, in which the properties of the system depend on the thermal history, is far less common and can be typically observed in a narrow temperature range around the first order phase transition temperature only [11], where a finite energy barrier exists between the high temperature and the low temperature state. In rare cases such hysteresis spans several decades in temperature [12]. Thermal hysteresis can also be observed at the glass transition [13], however this is essentially a dynamical phenomenon and depends strongly on the rate of temperature change.

The hysteresis in CDW systems does not fit in any of these categories. It is rate independent and occurs in a wide temperature range below the CDW transition

temperature [2, 5, 7, 8], down to the temperature of the glass transition in CDW superstructure [14, 15]. At any temperature within the hysteresis loop, the reversal of the temperature variation from cooling to heating (or heating to cooling) changes the value of the measured quantity from cooling to heating (heating to cooling) limiting curves already within 10 K [3–5, 7, 9]. Also, temperature cycling in ever smaller loops produces a stable state near the middle of the hysteresis loop [3]. The same state can be produced by applying an electric field above the threshold field for CDW sliding and the temperature evolution from this state is the same regardless of the way it is obtained [4]. Such a peculiar feature sets the thermal hysteresis in CDW systems apart from the hysteretic behaviour in other systems.

The origin of the thermal hysteresis in CDW systems has been attributed in [3, 4] quite generally to the hidden parameter which varies with the temperature and changes completely the free energy surface in the configuration space similarly as in the spin glasses [16]. Subsequent measurements of the hysteresis in very thin samples of o-TaS_3 [17] have shown that the temperature dependence of the dc resistivity $\rho_{dc}(T)$ consists of the regions with smooth variation interrupted by abrupt jumps. The direction of these jumps is always towards the interior of the hysteresis loop and they occur almost at the same temperatures on cooling and heating. It was concluded that this behaviour originates from the temperature dependence of CDW wavevector q_{CDW}. It is well established that from the transition temperature down to below 100 K q_{CDW} in o-TaS_3 and in $K_{0.3}MoO_3$ changes about 2% [18, 19]. However, the change of q_{CDW} cannot proceed uniformly [20], as there has to be an integer number of CDW wavelengths in the sample. Therefore, q_{CDW} will lag behind the equilibrium value q_{eq} and it will approach q_{eq} through quantized changes corresponding to the addition/removal of one CDW wavefront. It has been shown [20, 21] that these changes should occur locally, at the length scales of the order of the phase domain, through the phase slip process, i.e. the creation of topological defects in the CDW phase. Finite energy required for the phase slip implies also the hysteretic behaviour of q_{CDW} when cycling q_{eq} (and consequently the temperature). As the variation of q_{CDW} changes the free carrier density by adding or removing electrons from CDW condensate [22], the thermal hysteresis in q_{CDW} should result in the thermal hysteresis in the resistivity as well. In thin samples in which one phase domain can span the entire sample cross-section, the phase slip can therefore result in an abrupt jump in the resistivity.

The theory presented in the preceding paragraph aims at explaining the hysteretic behaviour in the free carrier conductivity of CDW systems. However, it implies that the hysteretic effects should be present in the properties of the CDW subsystem as well. On one hand, the phase slip process alters directly the phase configuration [20]. On the other, the free carriers screen the phase deformations [23, 24] and the change of free carrier density should affect the CDW subsystem. From this point of view it is interesting to study directly the properties of the CDW subsystem as a function of temperature cycling.

So far, the dielectric spectroscopy seems to be the most appropriate technique to probe directly the properties of CDW superstructure. It has enabled the observation of low frequency relaxation processes related to the localized phase dynamics [25, 26, 14, 15]. The high temperature, or α process [25] has been attributed to the correlated dynamics of phase domains and its temperature evolution is governed by the free carrier screening of the domain interactions [23, 24]. The freezing of the α process at a finite temperature [14, 15], at which its dynamics becomes too slow to be observed at the experimental timescales, implies the existence of the glass transition at the level of the CDW superstructure [14, 15]. The glass transition temperature T_g can be determined from the freezing criterion which states that the screening becomes ineffective when there is less than one free carrier per phase domain. T_g almost coincides with the low temperature endpoint of hysteresis. The low temperature, or β process [26] splits from the high frequency tail of the α process above T_g [14, 15] and becomes dominant below T_g. It has been attributed to the localized dynamics of the topological defects of the phase pinned at the impurities. The glass transition accounts naturally for the low temperature glass-like features [27]. Evidently, the dielectric spectroscopy can provide information on the influence of both the topological defects of the phase and the free carriers on the properties of the CDW superstructure. Therefore we have applied this method to investigate the hysteresis in CDW system o-TaS_3 in order to gain more insight in the nature of hysteretic effects.

2. Experimental details

The complex frequency dependent conductivity $\sigma(\nu) = \sigma' + i\sigma''$ of several o-TaS_3 samples from various batches has been measured in a wide frequency (ν) range from 100 MHz down to 100 Hz using an Agilent 4294A impedance analyzer. The whisker-like samples have been mounted at the end of the coaxial line, bridging the inner and the outer conductor and cooled using a closed-cycle refrigerator system [28]. Typical signal amplitude has been 5–30 mV, well within the linear response regime. The samples have been typically cooled from 300 K down to 20 K and than heated back to 300 K at various rates from 0.1 K min^{-1} up to 1 K min^{-1}. This temperature range extends sufficiently beyond the temperature range between the CDW transition temperature $T_P = 220$ K and the glass transition temperature $T_g \approx 50$ K [14] in which the thermal hysteresis in the DC conductivity is observed [2]. For given rates no temperature lag has been observed. In addition, several other temperature variation/cycling schemes have been used, such as the heating to 300 K and cooling back to 20 K after several days of annealing at 20 K, or performing smaller loops around 100 K. Whisker-like samples of various lengths from 2 mm up to 12 mm and cross-sections from 10^{-4} to 10^{-3} mm^2 produced quantitatively very similar results.

The dielectric function $\epsilon(\nu) = \epsilon' - i\epsilon''$ has been calculated from $\sigma(\nu)$ after subtraction of (real) dc conductivity σ_{dc} as

$$\epsilon(\nu) = \frac{\sigma(\nu) - \sigma_{dc}}{i2\pi\nu\epsilon_0} \qquad (1)$$

where ϵ_0 stands for the vacuum dielectric constant.

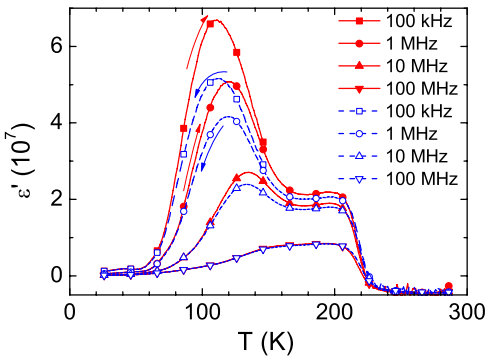

Figure 1. Temperature dependence of ϵ' measured on cooling and heating at selected frequencies. Arrows indicate the direction of temperature change. The data, taken at 1 K intervals, are presented with lines. The symbols are used to distinguish the curves for different frequencies. Solid lines and filled symbols correspond to heating and dashed lines and empty symbols correspond to cooling.

The dc conductivity remains quite high well in to the semiconducting region below T_P. It prevents accurate measurement of σ'' and therefore the determination of ϵ' at low frequencies.

3. Results and discussion

In figure 1 we present the temperature dependence of ϵ' at several frequencies measured during the temperature cycling from 300 to 20 K (cooling) and back to 300 K (heating) at 0.2 K min^{-1} rate. The ϵ' data at lower frequencies have been omitted due to large scattering above 100 K. The same results have been observed for the rates as different as 0.1 and 1 K min^{-1}. Global temperature dependence of ϵ' presented in figure 1 is well known for o-TaS_3 [25, 14]. The low frequency dielectric constant is negative at room temperature, reflecting the metallic state, and then becomes positive and relaxation-like below T_P, in the semiconducting CDW state, passing through a frequency dependent maximum around 100 K.

The dielectric constant exhibits a clear thermal hysteresis, reaching higher values on heating than on cooling. It appears in the temperature range slightly narrower than the region between the CDW transition temperature and the glass transition temperature. Particularly in the low temperature limit the hysteresis loop closes at higher temperatures for higher frequencies. In addition, the hysteresis loop width (ratio of heating and cooling values) decreases with increasing frequency.

The frequency dependence of ϵ' and ϵ'' measured on cooling and heating at selected temperatures is presented in figure 2. Evidently, the temperature cycling affects only the low frequency relaxation process (α process of [14]) which is dominant in the temperature range of the hysteresis. The β process [14, 26], which persists after the α process has frozen at T_g, is not affected, as seen in figure 2(b). As the temperature is lowered, the α process moves to lower frequencies, so the hysteresis loops for higher frequencies in figure 1 become narrower and open at higher temperatures only.

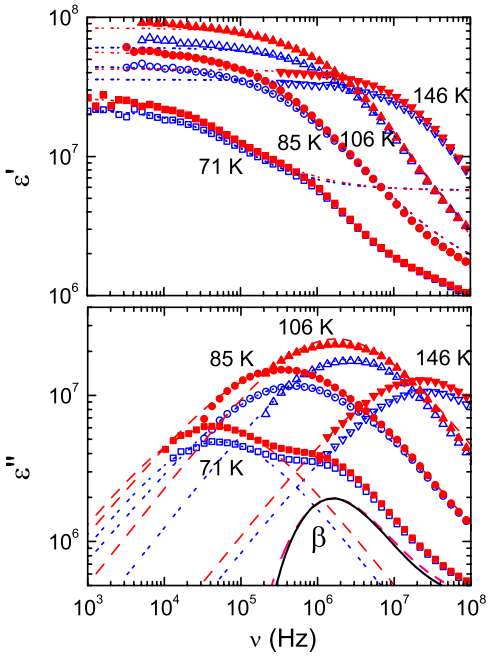

Figure 2. Frequency dependence of ϵ' and ϵ'' measured on cooling and heating at selected temperatures. Filled symbols are for heating and empty symbols for cooling. Dashed lines are fits of the α process to the Cole–Cole function. In (b) the fit at 71 K has been subtracted from the measured ϵ'' to reveal the β process only. It is presented with thick lines, solid for heating and dashed for cooling.

In addition to higher amplitudes, the α process also exhibits smaller relaxation frequencies (corresponding to the positions of the maxima of $\epsilon''(\nu)$ in figure 2(b)) on heating than on cooling. In order to quantify this difference, we have fitted $\epsilon(\nu)$ of the α process with the complex Cole–Cole function, which describes a symmetrically broadened Debye relaxation:

$$\epsilon(\nu) = \frac{\Delta\epsilon}{1 + (\mathrm{i}2\pi\nu\tau)^{1/w}} + \epsilon_\infty \qquad (2)$$

where $\Delta\epsilon$ represents the amplitude, τ the relaxation time and $1/w$ the inverse half-width of the relaxation process, while ϵ_∞ is the high frequency base line of ϵ'. The fits are given as dashed lines in figure 2. In figure 2(b) we have subtracted the fit at 71 K from the measured ϵ'' in order to demonstrate that the β process is not affected by temperature cycling. Below 70 K the accurate determination of $\epsilon(\nu)$, and therefore the characteristic parameters of the α process, below 10^4 Hz is not possible due to the high σ_{dc}.

The parameters $\Delta\epsilon$, τ and $1/w$ are presented in figure 3. Both the amplitude and the relaxation time of the α process are higher on heating. On the other hand, $1/w$, shown in the inset of figure 3 remains the same, demonstrating that the distribution of elementary processes is not affected by cycling.

As ϵ is proportional to the frequency dependent part of the conductivity $\sigma_{ac} = \sigma(\nu) - \sigma_{dc}$, it means that σ_{ac} is higher on heating than on cooling while it is well established that σ_{dc} is lower on heating. In order to emphasize this, we present in figure 4 the temperature dependence of σ' at selected frequencies measured in the same temperature run as the data in figure 1.

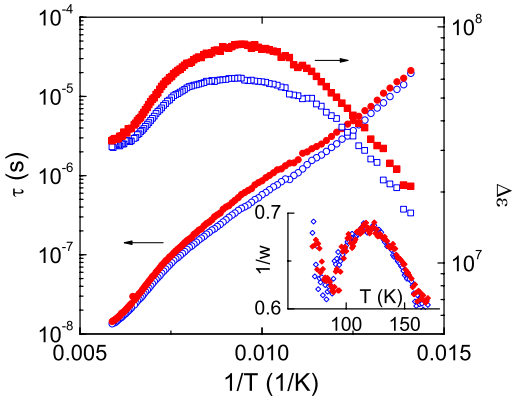

Figure 3. Temperature dependence of the Cole–Cole fit parameters $\Delta\epsilon$, τ and $1/w$ (in the inset) of the α process obtained on cooling and heating.

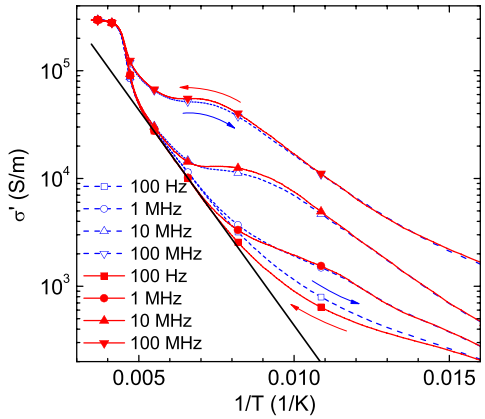

Figure 4. The Arrhenius representation of the temperature dependence of σ' measured on cooling and heating at selected frequencies. Arrows indicate the direction of temperature change. The data, taken at 1 K intervals, are presented with lines. The symbols are used to distinguish the curves for different frequencies. Solid lines and filled symbols correspond to heating and dashed lines and empty symbols to cooling. Straight solid line indicates the activated temperature dependence of σ_{dc} on heating below T_P.

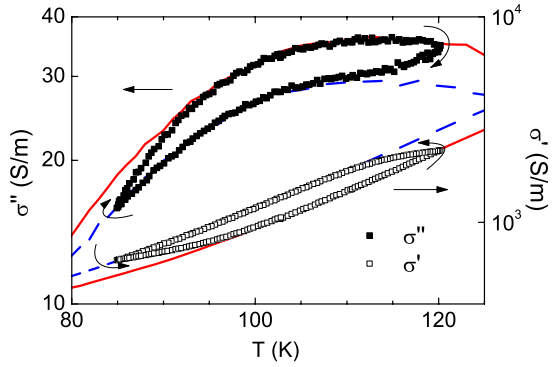

Figure 5. The temperature dependence of σ' and σ'' at 100 kHz obtained on the temperature cycling in the reduced range around 100 K. Arrows indicate the direction of temperature change. Thin lines represent the data, taken at 1 K intervals, obtained on heating (solid) and cooling (dashed) in the entire temperature range of the hysteresis.

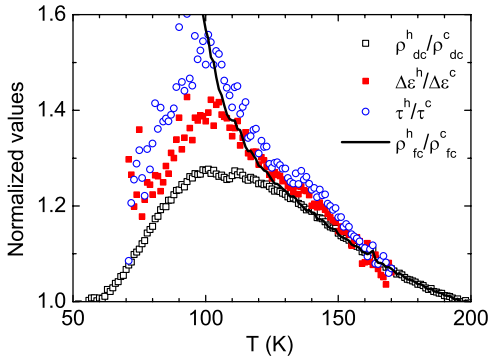

Figure 6. Temperature dependence of the normalized values (ratios of values obtained on heating and on cooling) of the amplitude, $\Delta\epsilon^h/\Delta\epsilon^c$, and the relaxation time, τ^h/τ^c, of the α process compared to the normalized values of dc resistivity, ρ^h_{dc}/ρ^c_{dc}, and the free carrier resistivity, ρ^h_{fc}/ρ^c_{fc} (see text for details on the estimate of ρ_{fc}).

The data of σ' at 100 Hz are identical to the measurements of σ_{dc} in 4 contact configuration, which proves that the contact contributions do not play any role. The conductivity is reduced at T_P due to the condensation of free carriers into the CDW state and decreases further with the temperature due to the opening of the gap. Below T_P, σ_{dc} follows the activated temperature dependence down to 120 K, $\sigma_{dc} = \sigma_0 \exp(-E_{act}/k_B T)$ with $E_{act} = 800$ K for cooling and 920 K for heating (shown in figure 4), and then deviates from it towards a plateau. The shoulders in $\sigma'(T)$ at higher frequencies correspond to the relaxation features seen already in $\epsilon'(T)$ in figure 1.

All curves show hysteretic behaviour to some extent. Hysteresis in σ_{dc}, which opens at 210 K, slightly below T_P, and closes at 55 K, slightly above T_g, is well known and extensively studied [2–4]. However, as the frequency increases, the hysteresis loops in σ' first become narrower and finally invert. The σ_{ac} dominates over σ_{dc} at high enough frequencies, so this is a natural consequence of the hysteresis loop in σ_{ac} inverted in respect to σ_{dc}.

Even if the hysteresis loops in σ_{ac} and σ_{dc} are inverted, they are still closely related. In figure 5 we present the data of σ' and σ'' at 100 kHz obtained on small temperature cycle around 100 K. The σ' at 100 kHz has a sufficiently small ac component, so that $\sigma' \approx \sigma_{dc}$, while σ'' does not have the dc component and $\sigma'' \propto \epsilon'$. Nevertheless, in these smaller loops the data fully reverse to the limiting cooling/heating curves within 10 K both in σ' and σ'', which suggests a strong coupling between these two values.

From the data presented in figure 3 it is clear that the temperature cycling affects only the α process in $\epsilon(\nu)$. Therefore it is reasonable to compare the hysteresis in the characteristic parameters of the α process only with the hysteresis in σ_{dc}. Actually, we use the dc resistivity $\rho_{dc} = 1/\sigma_{dc}$ as it is higher on heating, just as $\Delta\epsilon$ and τ. In figure 6 the normalized values (ratios of values obtained on heating and on cooling) of the amplitude, $\Delta\epsilon^h/\Delta\epsilon^c$, and the relaxation time, τ^h/τ^c of the α process are compared to the normalized value of dc resistivity, ρ^h_{dc}/ρ^c_{dc}.

All three normalized values have similar temperature dependences. At 170 K $\Delta\epsilon^h/\Delta\epsilon^c$ and τ^c/τ^h have the same value as ρ^h_{dc}/ρ^c_{dc}. As the temperature decreases, the hysteresis becomes more pronounced in $\Delta\epsilon$, and particularly in τ. Nevertheless, all normalized values pass through a maximum at about 100 K, which is very close to the temperature where $\Delta\epsilon$ has a maximum as well, see figure 3. While it was not possible to follow the temperature dependence of α process below 70 K for the reasons presented above, both $\Delta\epsilon^h/\Delta\epsilon^c$ and τ^h/τ^c show a clear tendency to the value of 1 near 50 K, or T_g, signifying the closing of the hysteresis in $\Delta\epsilon$ and τ.

Extensive work [23, 24] has been devoted to the explanation of the temperature evolution of the α process, particularly the thermally activated increase of τ with the decreasing temperature, which follows the thermally activated increase of ρ_{dc}. It has been concluded that the relaxation of the phase domains, i.e. the local CDW phase deformations, requires the redistribution of the free carriers in order to maintain the charge neutrality, so-called screening. Consequently, the relaxation frequency becomes proportional to the conductivity of the free carriers and therefore $\tau \propto \rho_{dc}$. Moreover, in [24] it has been argued that, due to the screening, the dielectric constant should increase with the increase of the free carrier resistivity as well. In this respect, the hysteresis in both $\Delta\epsilon$ and τ should follow the hysteresis in ρ_{dc}, which does not seem to be the case.

However, recent photoconductivity measurements [29] have demonstrated that below 100 K two channels contribute to the dc conductivity in o-TaS_3, just as suggested long time ago [30]. The one corresponding to the free carriers follows the activated dependence of σ_{dc}, presented in figure 4, down to 50 K. Below 100 K a new channel opens, which is responsible for the deviation from the activated dependence of σ_{dc}, again see figure 4, and corresponds to the contribution of collective excitations. The collective excitations should not contribute to the screening of phase deformations and therefore to the temperature dependence of ϵ. The τ of the α process should therefore follow the activated temperature dependence even below 100 K, exactly as it has been observed in [14].

In following we estimate the contribution to the hysteresis in σ_{dc} from free carriers only and compare it to the hysteresis in the characteristic parameters of the α process. We assume that contributions of free carriers (σ_{fc}) and collective excitations (σ_{coll}) to σ_{dc} are additive, $\sigma_{dc} = \sigma_{fc} + \sigma_{coll}$, and, according to the theory [22], that the thermal hysteresis is present only in σ_{fc}. In this case the normalized value of the free carrier resistivity, $\rho_{fc} = 1/\sigma_{fc}$, on heating and cooling can be roughly estimated as following [31]:

$$\frac{\rho^h_{fc}}{\rho^c_{fc}} = \frac{\sigma^c_{fc}}{\sigma^h_{fc}} = \frac{\sigma^c_{fc} - \sigma^h_{fc}}{\sigma^h_{fc}} + 1 = \frac{\sigma^c_{dc} - \sigma^h_{dc}}{\sigma^h_{fc}} + 1. \qquad (3)$$

We have obtained the difference $\sigma^c_{dc} - \sigma^h_{dc}$ directly from the data, while we have approximated the σ^h_{fc} with the activated dependence represented by the thick solid line in figure 4.

The ρ^h_{fc}/ρ^c_{fc} calculated this way is represented by the solid line in figure 6. It does not close near T_g and $\Delta\epsilon^h/\Delta\epsilon^c$ and τ^h/τ^c follow it closely down to 100 K. This result, although obtained under some assumptions, confirms that the free carrier screening is responsible for the temperature evolution of the phase dynamics corresponding to the α process, and therefore for the hysteresis in the dielectric response, at least down to 100 K.

The temperature evolution of the hysteresis in the dielectric response below 100 K, on the other hand, cannot be explained within the existing theories. We note that there is a characteristic temperature range around 100 K in which $\Delta\epsilon$ of the α process has a maximum, the β process appears and the normalized values of $\Delta\epsilon$ and τ on heating and cooling have maxima and deviate from the normalized values of ρ_{fc}, so all these phenomena might have a common origin.

There is an alternative way to explain the hysteresis in $\Delta\epsilon$ and τ. The ϵ is related to the spatial fluctuations of CDW phase and it has been shown that the low frequency ϵ as well as the relaxation time τ increase with the non-uniformity of the CDW phase i.e. with the increase of local CDW deformations [32]. The decrease of q_{eq} with temperature requires phase slips to occur in order that q_{CDW} could approach q_{eq}, so at low temperatures the CDW phase should be more deformed [20]. In this respect, at the same temperature the CDW phase is more deformed if the system has been heated to that temperature than if it has been cooled. However, in this case it would be expected that the distribution of elementary processes, represented roughly by the value of the inverse half-width $1/w$ changes as well, which is not the case. Also, as it is estimated in [20], the initial, strongly localized phase deformation after the occurrence of the phase slip relaxes over the length scale of the order of the phase coherence, i.e. the domain size. This can be interpreted as the simple addition or removal of one CDW wavefront within a single domain. In respect to the new CDW wavelength this would not create any new phase deformation and thus would not contribute to the change of the dielectric response.

4. Conclusion

In conclusion, we have observed thermal hystereses in the dielectric response of the CDW system o-TaS_3 in a wide temperature range between the CDW transition temperature and the temperature where the glass transition in the CDW superstructure has been determined. It occurs in the same temperature range as the well-known hysteresis in the dc conductivity, but the ac conductivity is higher on heating while, in contrast, dc conductivity is lower. Such behaviour is consistent with the exchange of electrons between the CDW condensate and free carriers during the variation of the CDW wavevector with temperature. Although the hysteresis in the dielectric response can be qualitatively understood from the variation of phase deformations with phase slips, a direct influence of the free carrier density on the dielectric response through screening offers a more quantitative explanation in a wide temperature range.

Acknowledgments

We acknowledge the support from Croatian MSES projects 035-0352827-2842 and 114-0352827-1370 and from the

Deutsche Forschungsgemeinschaft via the Sonderforschungsbereich 484, as well as the support from DAAD and Croatian MSES through the collaborative project. D Starešinić has been supported by the Alexander von Humboldt Foundation. We thank Professor R Thorne for supplying the samples.

References

[1] Monceau P (ed) 1985 *Electronic Properties of Inorganic Quasi-One-Dimensional Compounds* (Dordrecht: Kluwer Academic)
Grüner G 1988 *Rev. Mod. Phys.* **60** 1129
Grüner G 1994 *Density Waves in Solids* (New York: Addison-Wesley)
[2] Higgs W and Gill J C 1983 *Solid State Commun.* **47** 737
[3] Wang Z Z and Ong N P 1986 *Phys. Rev.* B **34** 5967
[4] Duggan D M and Ong N P 1986 *Phys. Rev.* B **34** 1375
[5] Xue-mei W and Dian-lin Z 1996 *Phys. Rev.* B **54** 1443
[6] Higgs A W 1985 *Charge Density Waves in Solids* ed G Hutiray and J Solyom (Berlin: Springer) p 422
[7] Smontara A, Biljaković K, Mazuer J, Monceau P and Levy F 1992 *J. Phys.: Condens. Matter* **4** 3273
[8] Golovnya A V, Pokrovskii V Ya and Shadrin P M 2002 *Phys. Rev. Lett.* **88** 246401
[9] Itkis M E, Emerling B M and Brill J W 1997 *Phys. Rev.* B **56** 6506
[10] Wadhawan V K 2000 *Introduction to Ferroic Materials* (Singapore: Gordon and Breach)
[11] Brokate M and Sprekels J 1996 *Hysteresis and Phase Transitions* (New York: Springer)
[12] Fujita W and Awaga K 1999 *Science* **286** 261
[13] Donth E 2001 *The Glass Transition* (Berlin: Springer)
[14] Starešinić D, Biljaković K, Brütting W, Hosseini K, Monceau P, Berger H and Levy F 2002 *Phys. Rev.* B **65** 165109
[15] Starešinić D, Hosseini K, Brütting W, Biljaković K, Riedel E and van Smaalen S 2004 *Phys. Rev.* B **69** 113102
[16] Binder K and Young A P 1986 *Rev. Mod. Phys.* **58** 801
[17] Borodin D V, Zaitsev-Zotov S V and Nad' F Ya 1986 *JETP Lett.* **43** 625
[18] Wang Z Z, Salva H, Monceau P, Renard M, Roucau C, Ayroles R, Levy F, Guemas L and Meerschaut A 1983 *J. Phys. Lett.* **44** L311
[19] Pouget J P, Kagoshima S, Schlenker C and Marcus J 1985 *J. Physique* **46** 1731
[20] Pokrovskii V Ya and Zaitsev-Zotov S V 1989 *Synth. Met.* **32** 321
[21] Littlewood P B and Rice T M 1982 *Phys. Rev. Lett.* **48** 44
[22] Artemenko S N, Pokrovskii V Y and Zaitsev-Zotov S V 1996 *JETP* **83** 590
[23] Littlewood P B 1987 *Phys. Rev.* B **36** 3108
[24] Baier T and Wonneberger W 1990 *Z. Phys.* B **79** 211
[25] Cava R J, Fleming R M, Dunn R G and Rietman E A 1985 *Phys. Rev.* B **31** 8325
Lyons W G and Tucker J R 1989 *Phys. Rev.* B **40** 1720
[26] Nad' F Ya and Monceau P 1995 *Phys. Rev.* B **51** 2052
[27] Odin J, Lasjaunias J C, Biljakovic K, Hasselbach K and Monceau P 2001 *Eur. Phys. J.* B **24** 315
[28] Böhmer R, Maglione M, Lunkenheimer P and Loidl A 1989 *J. Appl. Phys.* **65** 901
Schnider U, Lunkenheimer P, Pimenov A, Brand R and Loidl A 2001 *Ferroelectrics* **249** 89
[29] Zaitsev-Zotov S V and Minakova V E 2006 *Phys. Rev. Lett.* **97** 266404
[30] Takoshima T, Ido M, Tsutsumi K, Sambongi T, Honma S, Yamaya K and Abe Y 1980 *Solid State Commun.* **35** 911
Zhilinskii S K, Itkis M E, Kal'nova I Yu, Nad' F Ya and Preobrazhenskii V B 1983 *Sov. Phys.—JETP* **58** 211
[31] Pokrovskii V Ya, private communication
[32] Littlewood P B 1986 *Phys. Rev.* B **33** 6694